Supramolecular and base-induced singlet oxygen generation enhancement of a water-soluble phthalocyanine

Shaun M. Smith[1], Thais F. Abelha[2,3], David Limón[2,3], Mario Samperi[4,a†], Bunty Sharma[4,b†], Kristjan Plaetzer[5], Fabienne Dumoulin[6], David B. Amabilino[1,7], Lluïsa Pérez-García[2,3,4*]

[1]*School of Chemistry, GSK Carbon Neutral Laboratories for Sustainable Chemistry, University of Nottingham, Nottingham, NG7 2TU, United Kingdom*

[2]*Departament de Farmacologia, Toxicologia i Química Terapèutica, Facultat de Farmàcia i Ciències de l'Alimentació, Avda. Joan XXIII 27-31, Universitat de Barcelona, 08028 Barcelona, Spain.*

[3]*Institut de Nanociència i Nanotecnologia UB (IN²UB), Universitat de Barcelona 08028 Barcelona, Spain*

[4]*Division of Advanced Materials and Healthcare Technologies, School of Pharmacy, University of Nottingham, Nottingham NG7 2RD, UK*

[5]*Laboratory of Photodynamic Inactivation of Microorganisms, Department of Biosciences and Medical Biology, University of Salzburg, Hellbrunnerstrasse 34, 5020 Salzburg*

[6]*Acıbadem Mehmet Ali Aydınlar University, Biomedical Engineering Department, Ataşehir, Istanbul, Türkiye*

[7]*Institut de Ciència de Materials de Barcelona (ICMAB-CSIC), Campus Universitari, 08193 Bellaterra, Spain*

[a]*Present address: Istituto di Tecnologie Avanzate per l'Energia "Nicola Giordano" - CNR-ITAE, Messina, Italy*

[b]*Present address: Department of Chemistry, Centre for Advanced Studies in Chemistry, Panjab University, Chandigarh-160014, India*

Received date (to be automatically inserted after your manuscript is submitted)
Accepted date (to be automatically inserted after your manuscript is accepted)

ABSTRACT: Investigation into the reactive oxygen species (ROS) generating abilities of photosensitizers outside of *in-vitro*/*vivo* conditions is a crucial element in the wider study of photodynamic therapy (PDT) in clinical settings. Zinc(II) phthalocyanine tetrasulfonic acid (**ZnPcTS**) is a water-soluble photosensitizer which can generate ROS as singlet oxygen (SO) under irradiation in the red and far-red region of the electromagnetic spectrum. Incorporation of **ZnPcTS** into nano-fibres of a bis-imidazolium hydrogel was demonstrated and the material characterized with photophysical, rheological, and microscopy techniques. This supramolecular material containing **ZnPcTS** (named **ZnPcTS_*n*EqBase@Gels**) was found to significantly enhance the SO generation rate with respect to that of **ZnPcTS** in aqueous solution. The effect is attributed mainly to reduced aggregation within the gel microenvironment compared with solution. Furthermore, the preparation of **ZnPcTS_*n*EqBase@Gels** was carried out in the presence varying amounts (0, 1, 2, 3, 4 eq.) of NaOH to improve dissolution of **ZnPcTS** by ensuring full deprotonation of the sulfonate. The gel material containing 4

equivalents of NaOH per phthalocyanine was found to have a significantly greater SO generating ability than the corresponding material containing no base. This phenomenon was shown to be partially a consequence of reduced aggregation as observed in the spectroscopic characterization. The enhancement in SO generation induced by this type of hybrid material makes it an attractive candidate to be used in different applications when efficient SO production is required.

KEYWORDS: Metal phthalocyanine, singlet oxygen, aggregation, supramolecular, hydrogel, fluorescence

*Correspondence to: mlperez@ub.edu. Departament de Farmacologia, Toxicologia i Química Terapèutica, Facultat de Farmàcia i Ciències de l'Alimentació, Avda. Joan XXIII 27-31, Universitat de Barcelona, 08028 Barcelona, Spain. Telefone: +34 934035849

†Present address: [a]Istituto di Tecnologie Avanzate per l'Energia "Nicola Giordano" - CNR-ITAE, Messina, Italy. Present address: [b]Department of Chemistry, Centre for Advanced Studies in Chemistry, Panjab University, Chandigarh-160014, India

INTRODUCTION

Amongst the porphyrinoid class of dyes, phthalocyanines have distinctive properties that make them suitable for several applications. They have been described by Tomás Torres and his co-workers as "old dyes, new materials" appropriate for "putting color in nanotechnology" [1]. As photo- and electro-active systems [2], they have been used in light harvesting materials such as dyes-sensitized solar cells [3], with the phthalocyanine TT1 being a key player in the field [4], and in hole- and electron-transporting materials for perovskite solar cells [5].

Their incorporation into advanced materials can be either based on supramolecular interactions or on covalent bonds [6-8], thanks to their nearly infinite structural variations [9]. Their maximum absorption (usually centred at 700 nm) is within the first phototherapeutic window, which is especially relevant for biomedical light management [10] and particularly photodynamic therapy (PDT) [11-12]. Several strategies to produce water-soluble phthalocyanines for biomedical applications have been developed in recent decades [13], and many sulfonated derivatives have been reported [14-15], usually with Zn or Al metal ions at their core to promote efficient singlet oxygen (SO) generation [16-18].

Beyond conferring water-solubility, the sulfonate substitution pattern, due to their negative charges, has been used to promote electrostatic interactions of phthalocyanines with various substrates and materials, for example polyethylenimine to form nano complexes with improved cellular internalization efficiency and phototoxicity [19], electrostatic self-assembled layer by layer films containing graphene oxide [20], cationic porphyrins [21], or biological components such membranes [22] or low-density lipoprotein [23].

An unexplored partner for the anionic phthalocyanines are gemini-type bis-imidazolium amphiphiles. These amphiphiles are versatile materials that have been successfully used for drug delivery [24, 25], as a supramolecular system for molecular walkers [26] and as SO enhancers for PDT [27]. In this latter example, the photosensitizer was incorporated into the hybrid nanomaterial through charge complementarity.

In this work, we report on the association of zinc(II) phthalocyanine tetrasulfonic acid (**ZnPcTS**) with a bis-imidazolium gel supramolecular platform capable of enhancing the photodynamic capability of the previous porphyrin-based photosensitizer [27]. We compared the photodynamic perfomance of **ZnPcTS** and its corresponding sulfonate salt (formed by deprotonation by NaOH) embedded into bis-imidazolium gels. Overall, we show that both **ZnPcTS** and its related salt were successfully encapsulated into bis-imidazolium gels and that distinct **ZnPcTS** structures influenced the physico-chemical characteristics of the photosensitizer-gel system. Most importantly, the **ZnPcTS** salt displayed improved reactive oxygen species (ROS) generation capability than the non-ionic **ZnPcTS** both in solution and in the fibres formed in the gel state.

EXPERIMENTAL

Synthesis

Commercially available reagents purchased from Sigma Aldrich, Acros Organics and Fisher Scientific were used without further purification. Preparation of the dicationic amphiphile gelator (**1.2Br**) was carried out through an established synthetic procedure [28].

Preparation of Gels

Unless explicitly stated otherwise, gels were prepared at a 1:1 water-ethanol ratio with a final gelator concentration of 12 mM. A total of five aqueous **ZnPcTS** 2.4 mM stock solutions (containing 0, 1, 2, 3, 4 eq. of NaOH relative to the concentration of **ZnPcTS**) were prepared to achieve the desired concentration in the gel. For the **1.2Br** gels, an equal volume of 24 mM gelator solution in absolute ethanol was added to the diluted **ZnPcTS** solution in MilliQ water (including NaOH where noted) *via* micropipette and mixed vigorously and rapidly. This preparation led to robust gels which were stable over the timescale of months at room temperature (approximately 18-25 °C).

Characterization of Gels

The rheological assessment of gel samples was performed in a HAAKE RheoStress 1 rheometer (Thermo Scientific) according to the procedure described previously [29]. Briefly, a sensor with 60 mm diameter (PP60) was used with a 3 mm gap between plates and the characterization was performed at 36 ± 1 °C. For the oscilatory amplitude sweep test, the amplitude of deformation (shear stress) was varied (0-100 Pa) while the frequency was kept constant at 1 Hz; while for the frequency sweep test, the shear frequency was varied (10.00 – 0.01 Hz) and the amplitude of the shear stress was set at 0.50 Pa. UV-Vis absorption spectroscopy measurements were taken with quartz cuvettes of path length 10 mm or 1 mm in a Cary UV-Vis NIR Spectrometer. Absorption measurements of gel samples containing **ZnPcTS** had to contain the photosensitizer at a higher concentration than samples used in the singlet oxygen studies to be able to see through the heavy scattering brought about by the gel. Fluorescence emission of gel (1 mm cuvette) and solutions (10 mm cuvette) was characterized using a FLS 980 spectrometer (Edinburgh Instruments) equipped with a front face sample holder. For gel fluorescence measurements, the use of long pass filters and front face geometry allow to remove the effect of scattering (the beam hits the cuvette surface and enters the detector). Fourier-transform infrared spectroscopy (FT-IR) was carried out on a Bruker Tensor 27 instrument equipped with a Pike GladiATR attachment with a diamond crystal and was performed in dried gel samples. SEM images were acquired with a JEOL 7100F FEG-SEM system on samples cast on aluminium stubs, dried under vacuum and coated with a 5-nm-thick layer of iridium. Image acquisition was performed using a working distance of 6 mm and 10 kV accelerating voltage.

Singlet Oxygen Measurements

SO generation was measured by monitoring the fluorescence decrease of 9,10-anthracenedyl-bis(methylene)dimalonic acid (**ABMA**) in water with the presence of **ZnPcTS** and **ZnPcTS_*n*EqBase@Gels** upon irradiation. The sample in a 10-mm

quartz cuvette was irradiated for 1-minute intervals using a diode laser of a 660 nm wavelength. The **ABMA** fluorescence was characterized using a FLS 980 spectrometer. In a typical SO experiment, a 0.5 mL sample of gel containing the **ZnPcTS** at a concentration of 10 μM was prepared in a syringe which, upon gelation, was dispersed into to 2 mL of a 146 μM **ABMA** solution to yield a suspension with a final working concentrations of 2 μM (**ZnPcTS**), 117 μM (**ABMA**) and a final ethanol content of 10% in 2.5 mL sample volume. Two SO generation experiments were carried out and the average emission decay of **ABMA** plotted as a function of irradiation time. All **ABMA** decay curves were fit to pseudo first order kinetics (**Eq. 1**) to determine rate constants.

$$(\boldsymbol{Eq.1})\ [\boldsymbol{A}] = [\boldsymbol{A}]_{\boldsymbol{0}} * \boldsymbol{e}^{-\boldsymbol{kt}}$$

RESULTS AND DISCUSSION

Gel preparation and characterization

The gels comprising the gelator, phthalocyanine and base - abbreviated **ZnPcTS_*n*EqBase@Gels** - were prepared using the solvent switch method where **1.2Br** in ethanol was added to the colorant solution in water (with NaOH where applicable) to give a mixture with a 1:1 water-ethanol ratio and a final **1.2Br** concentration of 12 mM within the gel as displayed in **Fig. 1**. In order to investigate the effect of **ZnPcTS** incorporation in the gel as the tetrasulfonic acid and as the corresponding salt derivative, stock solutions which contained 0-4 equivalents of NaOH relative to **ZnPcTS** (0 to 1 equivalent per sulfonic acid group). Gels prepared with *n* equivalents of NaOH are subsequently labelled **ZnPcTS_*n*EqBase@Gel**. After the mixture of the aqueous and ethanolic solutions, gelation generally occurred within one minute irrespective of the concentrations of **ZnPcTS**. No appreciable difference in gelation time was observed between the gels containing differing concentrations of NaOH and the prepared gels were both robust and stable over several months at room temperature.

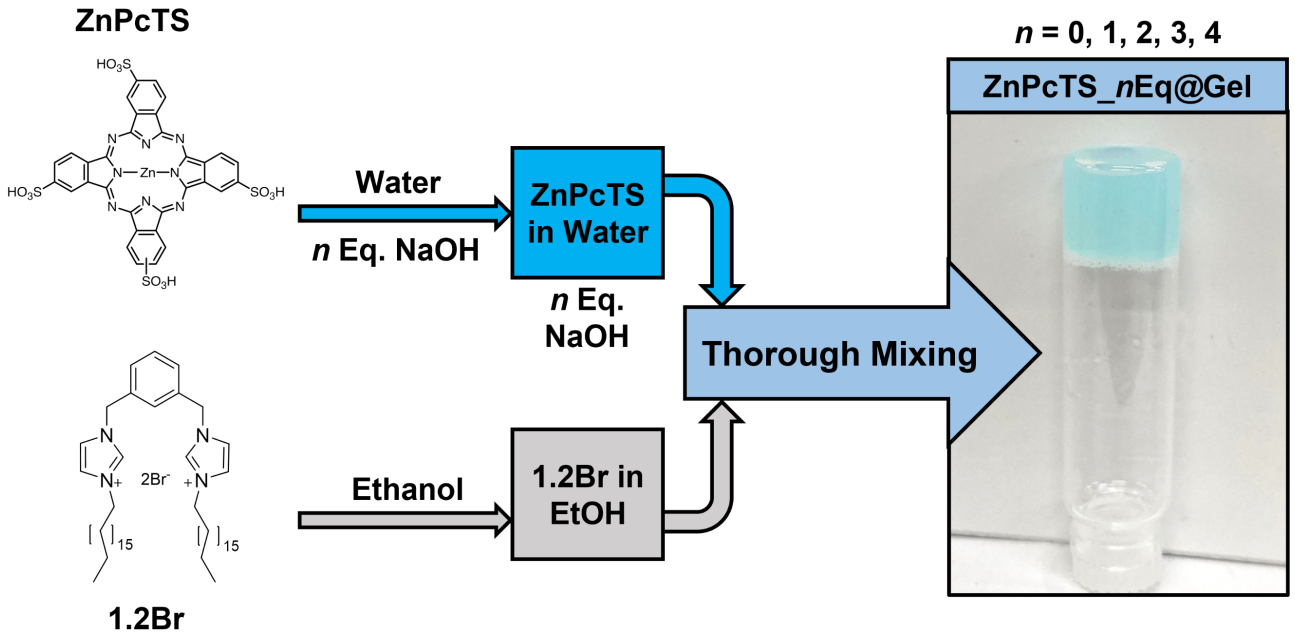

Fig. 1. Procedure for preparation of gels from an equal volume of **ZnPcTS_*n*EqBase@Gel** in water and **1.2Br** in ethanol.

FT-IR spectra of the pristine **1.2Br** xerogel (dried gel), **ZnPcTS_0EqBase@Gel** and **ZnPcTS_4EqBase@Gel** xerogels were collected and compared with **ZnPcTS** in the solid state are shown in **Fig. 2**. Xerogels were formed *via* drying a sample of the hydrated gel overnight under vacuum. The O-H stretch of the sulfonic acid found at 3205 cm^{-1} in the spectrum of the solid state **ZnPcTS** is not seen to the same extent in the **ZnPcTS_*n*EqBase@Gel**. The lack of a strong O-H stretch in the **ZnPcTS_0EqBase@Gel** xerogel indicates that there is a degree of deprotonation of the sulfonic acid groups even without the addition of base, at least in the dried form of the gel. Another characteristic peak is found at 1403 cm^{-1} and corresponds to the S=O stretch, which is not seen in the **1.2Br** xerogel spectrum, thus corresponding to the encapsulated phthalocyanine.

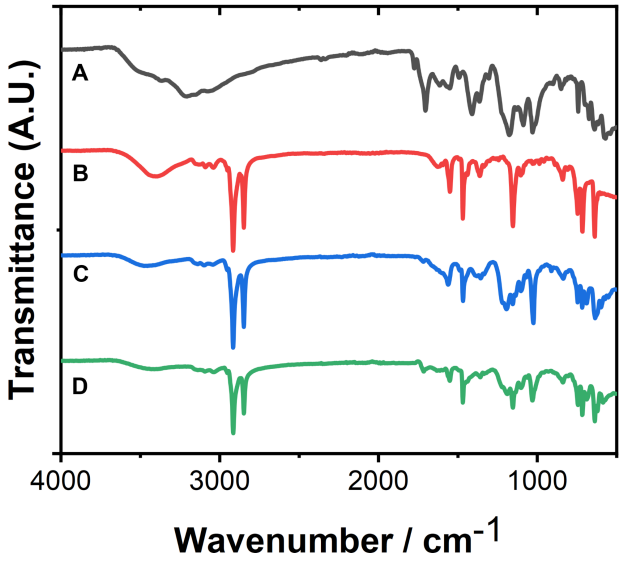

Fig. 2. FT-IR comparison of solid state **ZnPcTS**, pristine **1.2Br** xerogel and **ZnPcTS** xerogels. (**A**) Solid state **ZnPcTS**. (**B**) Pristine **1.2Br** xerogel, [**1.2Br**] = 12 mM, 1:1 water ethanol. (**C**) **ZnPcTS_4EqBase@Gel** xerogel, [**1.2Br**] = 12 mM, 1:1 water ethanol, [**ZnPcTS**] = 100 μM, [NaOH] = 400 μM. (**D**) **ZnPcTS_0EqBase@Gel** xerogel, [**1.2Br**] = 12 mM, 1:1 water ethanol, [**ZnPcTS**] = 100 μM. All concentrations are the final concentrations within each dried gel.

To better understand the microscale structure of the newly formed gels, SEM imaging was employed. **ZnPcTS_*n*EqBase@Gel** xerogel samples were prepared with no base and increasing concentrations of **ZnPcTS** (0 mM; 0.012 mM; 0.12 mM and 1.2 mM) with the gelator concentration kept constant at 12 mM. Further samples were prepared with the same concentrations of **ZnPcTS** but also including 4 eq. of NaOH to investigate the potential effect of base upon the microscale structure. SEM images (**Fig. 3**) reveal that when no **ZnPcTS** is present within the gels, the gel fibers are relatively well-defined, irrespective of the presence of base. Increasing the **ZnPcTS** concentration to 0.012 mM within the gel does not influence the fibers to a large extent. However, upon increasing to 0.12 mM and finally 1.2 mM, significant changes to the fiber morphology occur, moving from predominantly straight fibres (**Fig. 3A-D**) and upon increasing **ZnPcTS** loading, beginning to appear less straight and well-defined and cluster into areas of high fiber density (**Fig. 3E-H**). This trend towards greater morphological disturbance with greater photosensitizer loading is observed also with identical concentrations of a tetracarboxylated porphyrin [27].

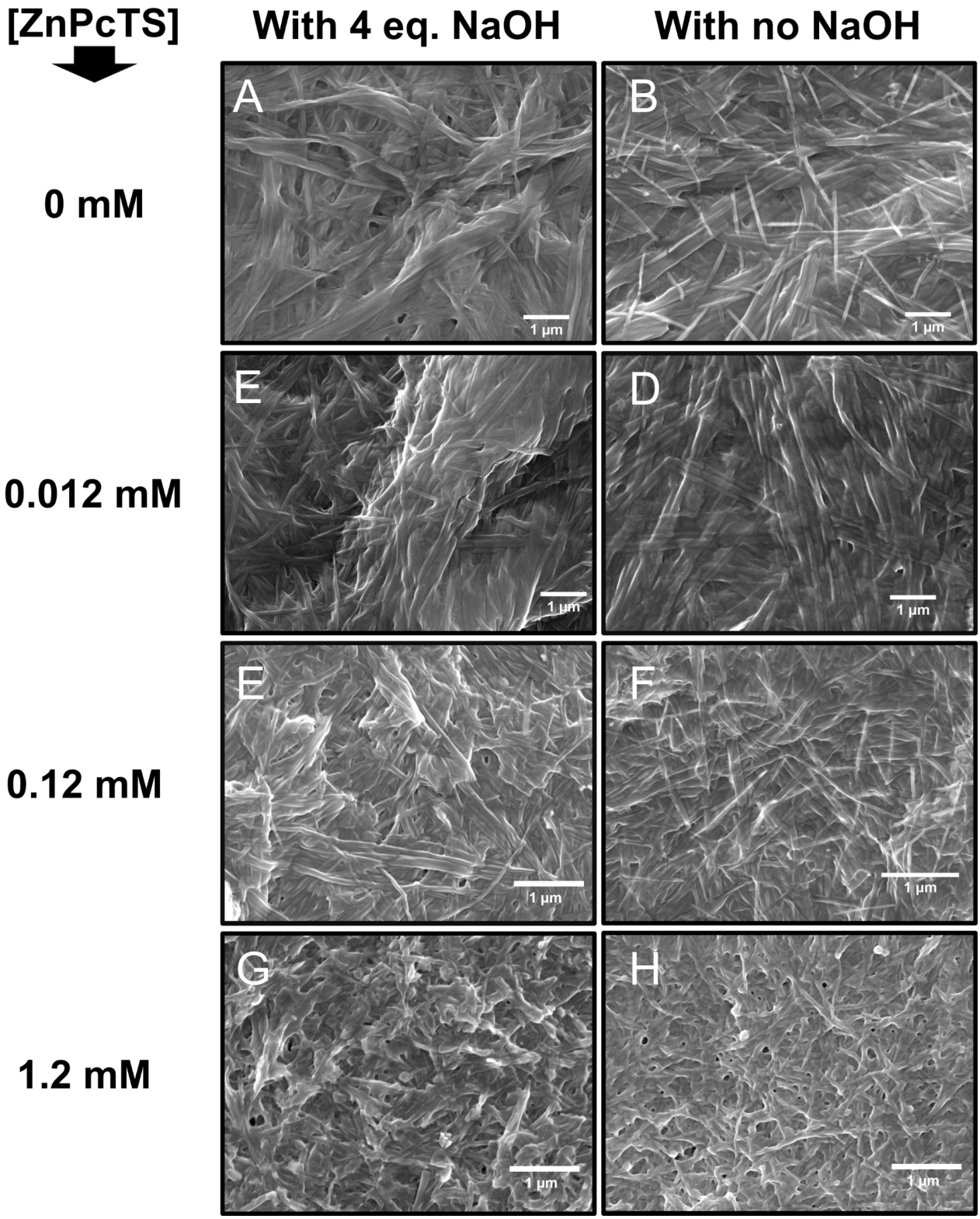

Fig. 3. SEM images xerogels of **1.2Br** gels formed in a 1:1 water-ethanol ratio and covered with a 5-nm-thick layer of iridium. **ZnPcTS** concentration is increased by a factor of ten until the final concentration of 1.2 mM. No discernible difference is observed between the samples containing 4 eq. and no base. Scale corresponds to 1 μm.

Rheological characterisation (**Fig. 4**) revealed the prevalence of the storage modulus (elastic modulus, G') over the loss modulus (G''), indicating that **1.2Br** gels have solid-like feature rather than a liquid behaviour independently of the presence of the phthalocyanine, which is in agreement with our previous reports on other guests in the gel [24, 26]. The incorporation of the **ZnPcTS** or the corresponding salt form increased both the gel resistance to deformation and the resistance to rupture, observing a greater influence in the case of **ZnPcTS** rather than the corresponding salt form. The increased resistance to deformation (G' and G'' values) and the increased resistance to rupture (Critical stress values) are shown in **Table 1**. We have previously shown that an increasing loading of a tetracarboxylated porphyrin within a **1.2Br** framework was correlated to an augmented resistance to rupture [27]. In this work, we report that phthalocyanines can induce a similar effect, but to a lower extent for the organic salt. There is a distinct contribution of the ionic and non-ionic **ZnPcTS** structure on the **1.2Br** gel assembly that affects the gel strength.

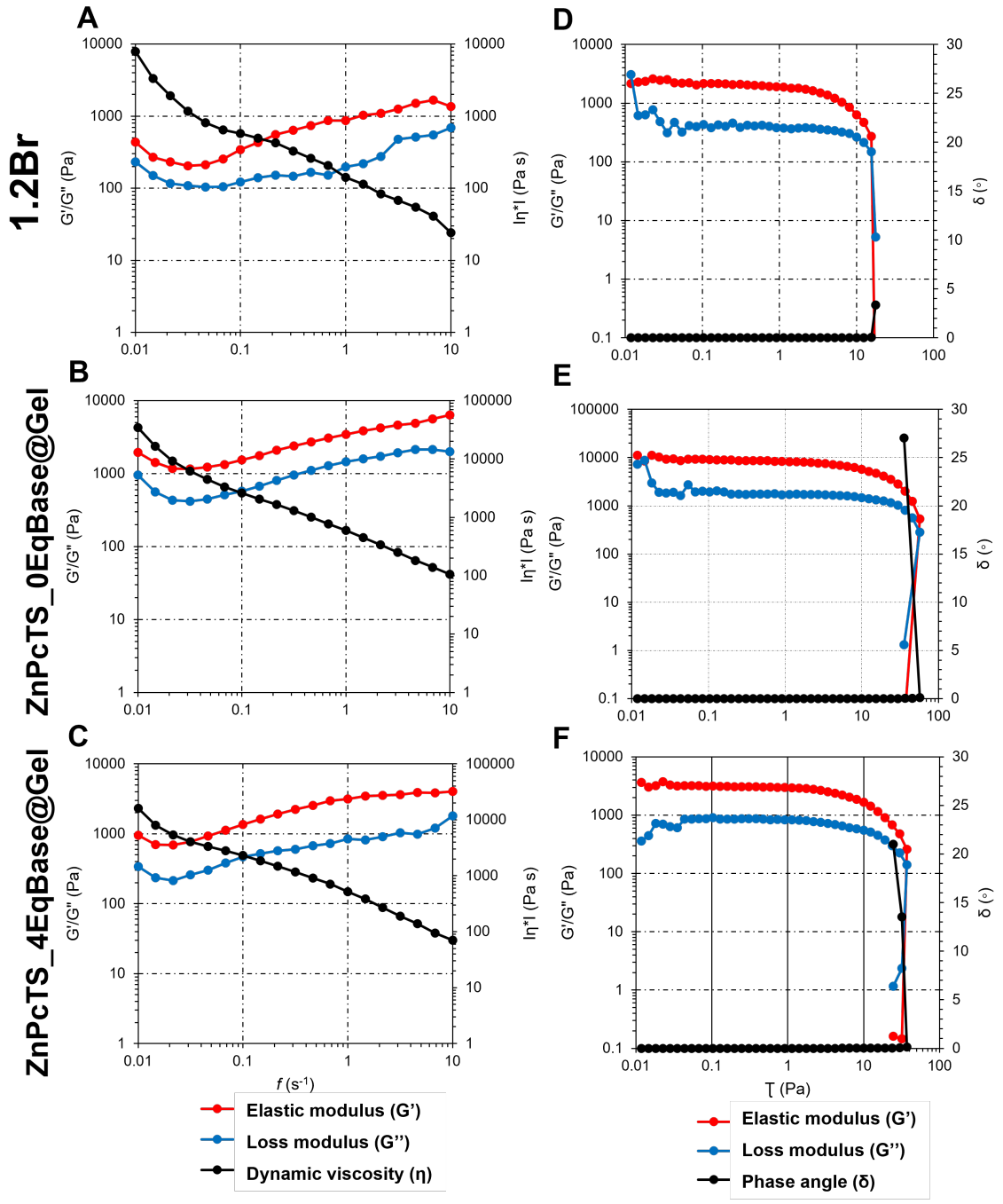

Fig 4. Frequency sweep (**A**, **B**, **C**) and amplitude sweep (**D**, **E**, **F**) profiles of **1.2Br** gel (**A**, **D**), **ZnPcTS_0EqBase@Gel** (**B**, **E**) and **ZnPcTS_4EqBase@Gel** (**C**, **F**).

Table 1. Critical stress values from oscillation amplitude sweep (crossover points when G' = G'').

Sample	G'*	G''*	Critical stress (Pa)
1.2Br gel	2059	410	15.52
ZnPcTS_0EqBase@Gel	8707	1808	57.02
ZnPcTS_4EqBase@Gel	3072	859	37.04

*Denotes average values at the linear viscoelastic region (0.1-1.0 Pa)

UV-Visible absorption and fluorescence spectroscopies

Phthalocyanines are generally susceptible to aggregation as a result of the stacking of their largely flat macrocycle cores. **Fig. 5A** displays the absorption spectrum of **ZnPcTS** in water (with and without 4 eq. NaOH) and in DMSO. The lack of **ZnPcTS** aggregation in DMSO is evidenced by the sharp peak at 679 nm, which corresponds to the non-aggregated **ZnPcTS** absorption maximum. The absorption spectrum of **ZnPcTS** in water without NaOH shows a Q-band centred at ~ 636 nm, and that of **ZnPcTS** in water with NaOH reveals a similar Q-band shape similar to the spectrum without base but containing a shoulder at ~ 679 nm. This observation indicates a lesser degree of aggregation of **ZnPcTS** in the presence of NaOH. The difference in aggregation tendency observed in solution is likely brought about by electrostatic interactions between the sodium cations and the anionic sulfonate group present upon the exterior of **ZnPcTS** in the presence of NaOH, and potential hydrogen bonding between sulfonic acid groups of neighbouring phthalocyanines without the presence of NaOH. The pKa of the **ZnPcTS** sulfonic acids can be estimated to be *ca*. -2 [30, 31] and therefore we expect that the protons are largely dissociated in neutral water. Indeed, the fact that the molecule incorporates into the gels is a clear indication of this fact, and the IR does not show the OH groups significantly (**Fig. 2**). We cannot be sure that in the aggregates in water that all of the acid protons will dissociate because of the local environment in the assembly, and it might be that hydrogen bonding between neighbouring stacked phthalocyanines takes place, and for this reason the addition of the base has such a large impact upon the absorption and fluorescence characteristics of the phthalocyanine. This aggregation also has the effect of quenching fluorescence emission of **ZnPcTS** in aqueous solution which can be seen in **Fig. 5B**, where the fluorescence emission spectra of **ZnPcTS** in DMSO and in water (with and without 4 eq. NaOH) is shown. As a result of the short lifetime of the second excited singlet state of **ZnPcTS**, only one significant emission peak resulting from the first excited state is observed when exciting the Soret band (~ 350 nm) or the Q-band in the red to far-red region (600-700 nm). A very shallow peak between 500-550 nm is seen with **ZnPcTS** in DMSO and corresponds to the minimal emission from the second excited state brought about by its short lifetime. Although relative fluorescence intensities between samples cannot be quantitatively compared, **ZnPcTS** in DMSO results in a significantly larger fluorescence than **ZnPcTS** in aqueous solution. The position of the emission maxima also varies depending on both solvent and presence of base. The emission maximum of **ZnPcTS** in DMSO is located at 695 nm, and that of **ZnPcTS** in water (with and without 4 eq. NaOH) is present at 685 nm and 691 nm, respectively.

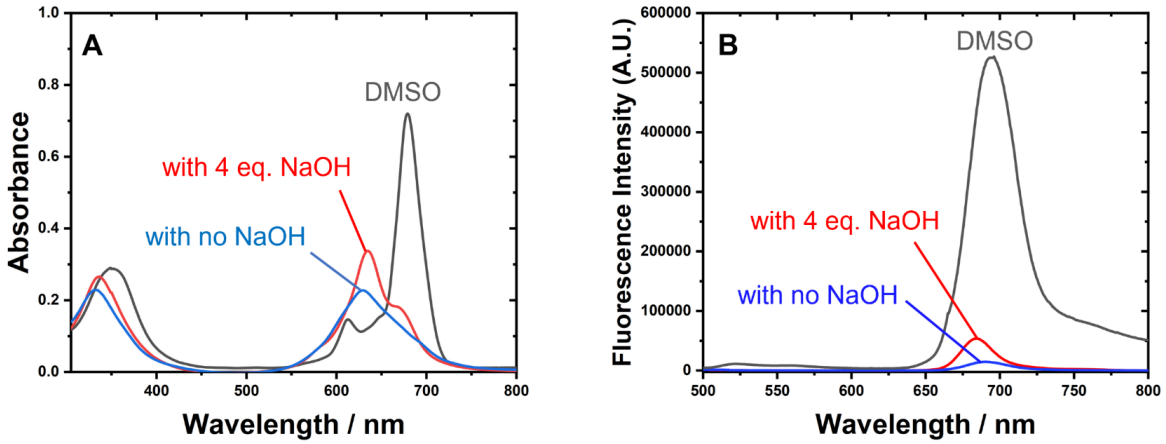

Fig. 5. (**A**) Absorption spectrum of **ZnPcTS** at a concentration of 10 μM in DMSO (black), water with 4 eq. NaOH (red), and water without NaOH (blue). (**B**) Fluorescence emission spectrum of **ZnPcTS** at a concentration of 10 μM in DMSO (black), water with 4 eq. NaOH (red), and water without NaOH (blue). $\lambda_{exc.}$ = 300 nm and λ_{filter} = 330 nm for all three measurements.

Another commonly used method to prevent aggregation of hydrophobic core-containing molecules is to introduce surfactants into the system. Cetrimonium bromide (**CTAB**) (shown in **Fig. 6A**), a cationic surfactant, has been shown to inhibit aggregation in water-soluble phthalocyanines [32]. **Fig. 6** shows the absorption spectra of **ZnPcTS** in water with 4 eq. NaOH (**Fig. 6A**) and in water without NaOH (**Fig. 6B**). In each spectrum, the effect of increasing the **CTAB** concentration from 0 to 1 μM to 10 μM can be seen. The effect of disaggregation that can be seen by the increase of the **ZnPcTS** monomer Q-band at ~ 679 nm is observed both in the presence of base and without, but is more pronounced in the solutions containing 4 equivalents of NaOH. This disparity in effect is probably a consequence of the anionic character of the deprotonated **ZnPcTS** and its more significant interaction with the cationic **CTAB**. As seen from the fluorescence emission spectra (**Fig. 6C**), fluorescence intensity increases (as predicted) with the addition of **CTAB** at a concentration of 1 μM but is almost completely quenched at a concentration of 10 μM. This complete reduction of fluorescence could be result of the heavy atom effect brought about by the bromide anions, which have been shown to reduce the fluorescence of anthracene derivatives by increasing their triplet state lifetimes [33].

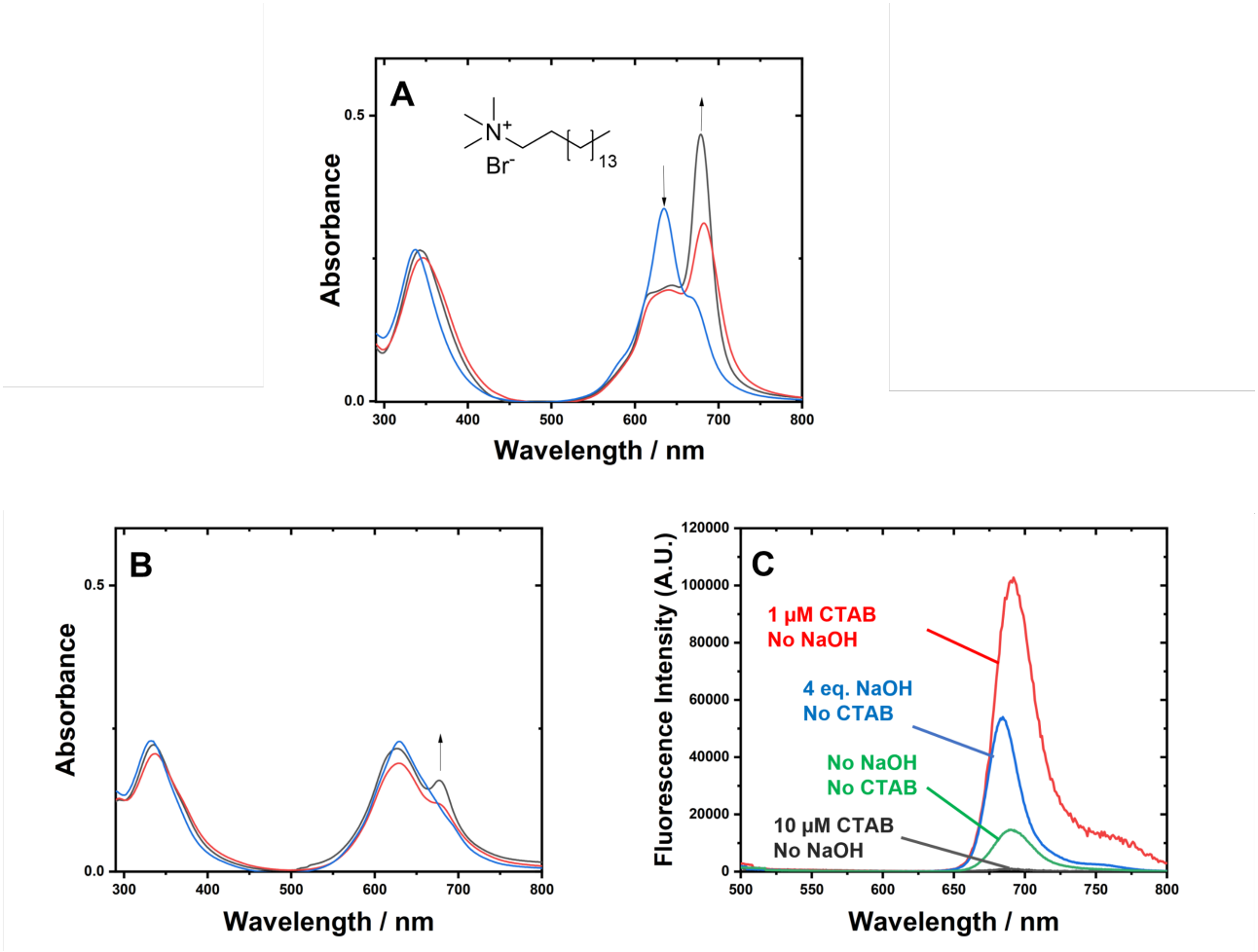

Fig. 6. (**A**) Absorption spectra of **ZnPcTS** (10 μM) with 4 eq. NaOH containing no **CTAB** (blue), 1 μM **CTAB** (red), and 10 μM **CTAB** (grey). **CTAB** structure shown. (**B**) Absorption spectra of **ZnPcTS** (10 μM) with no NaOH containing no **CTAB** (blue), 1 μM **CTAB** (red), and 10 μM **CTAB** (grey). (**C**) Fluorescence emission spectra of **ZnPcTS** (10 μM) with no NaOH and no **CTAB** (green), with 4 eq. NaOH and no **CTAB** (blue), with no NaOH and 1 μM **CTAB** (red), and with no NaOH and 10 μM **CTAB** (grey). λ_{exc} = 300 nm and λ_{filter} = 330 nm for all fluorescence measurements.

The absorption characteristics of **ZnPcTS** when incorporated into the gel were also were influenced by the presence of NaOH. **Fig. 7A** shows the absorption spectra of **ZnPcTS_4EqBase@Gel** and **ZnPcTS_0EqBase@Gel**. **ZnPcTS_4EqBase@Gel** has a greater attenuation coefficient in the Q-band region than **ZnPcTS_0EqBase@Gel** along with a different Q-band shape. This disparity in absorbance could be explained by the varying extents of aggregation of **ZnPcTS** within the gel with and without the presence of base. Fluorescence emission spectra (**Fig. 7B**) of gels containing an intermediate amount (1, 2, 3 eq. NaOH) of base show an initial decrease in emission intensity and a bathochromic shift in the position of the emission maximum from 0 to 1 eq. of NaOH, followed by hypsochromic shifts from 1 to 4 eq. NaOH. This decrease in fluorescence intensity upon the addition of 1 equivalent of NaOH was not expected, as lowering aggregation tends to increase fluorescence activity, though this result is discussed further in the context of the singlet oxygen generation experiments. In order to mimic the solvent composition within the gel, the absorption and emission spectra of **ZnPcTS** in 1:1 water-ethanol solution were characterized (**Fig. 7C**,**D**). Again, **ZnPcTS** in the presence of base in this 1:1 water-ethanol solution exhibits greater absorbance and an attentuation coefficient which is more than double that of **ZnPcTS** in 1:1 water-ethanol without the presence of base. The Q-band of **ZnPcTS** with 4 eq. NaOH in 1:1 water-ethanol strongly resembles that of **ZnPcTS** in DMSO,

indicating that the **ZnPcTS** is not aggregated in 1:1 water-ethanol when 4 eq. of NaOH are present. When base is not present, the Q-band shape is more complex with the two peaks split into four. This Q-band splitting pattern is observed in the free base phthalocyanine H_2Pc but also seen in metalated phthalocyanines [34]. Absorption spectra of **ZnPcTS@Gel** samples containing 1-3 equivalents of NaOH show intermediate Q-band shapes between that of the 0 eq. and 4 eq. NaOH samples. The attenuation coefficients and absorption maxima of **ZnPcTS** in solution/gel (**Table 2**) reveal that **ZnPcTS** with 4 eq. NaOH possesses a higher absorption than that of the counterpart without NaOH.

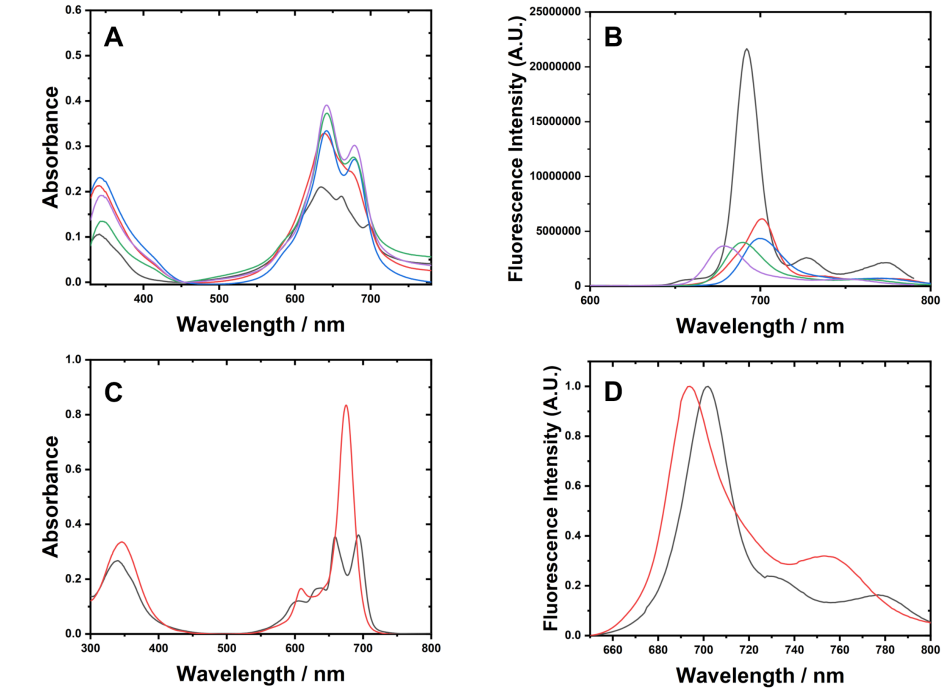

Fig. 7. (**A**) Absorption spectra of **ZnPcTS_*n*EqBase@Gels**, $n = 0$ (grey), $n = 1$ (red), $n = 2$ (blue), $n = 3$ (green), $n = 4$ (lilac), [**ZnPcTS**] = 100 μM. (**B**) Fluorescence emission spectra of **ZnPcTS_*n*EqBase@Gels**, $n = 0$ (grey), $n = 1$ (red), $n = 2$ (blue), $n = 3$ (green), $n = 4$ (lilac), [**ZnPcTS**] = 10 μM. (**C**) Absorption spectra of **ZnPcTS** (10 μM) in 1:1 water-ethanol with 4 eq. NaOH (red) and no NaOH (grey). (**D**) Fluorescence emission spectra of **ZnPcTS** (10 μM) in 1:1 water-ethanol with 4 eq. NaOH (red) and no NaOH (grey). λ_{exc} = 625 nm and λ_{filter} = 645 nm for these fluorescence measurements.

Table 2. Attenuation coefficients of **ZnPcTS** in different systems.

	Attenuation Coefficient (**ε**)		
ZnPcTS_*n*EqBase	Water	1:1 Water-Ethanol	1.2Br Gel
***n* = 4**	34000	83000	39000
***n* = 0**	22000	36000	21000

Singlet oxygen generation

The SO-generating ability of the gels was assessed using **ABMA**, a fluorescent probe which reacts with singlet oxygen producing a non-fluorescent (in visible spectrum) endoperoxide compound and reducing the overall **ABMA** fluorescence emision between ~ 400 – 500 nm [35]. A diode laser of 660 nm was used to excite the Q-band of **ZnPcTS**, and subsequently generate SO. A comparison of the **ZnPcTS** in solution and within the gel would confirm whether disaggregation had a considerable effect upon the SO generating ability, along with how the presence of base influences SO generation. **Fig. S1A**

shows overlaid fluorescence spectra of **ABMA** over fifteen minutes of irradiation in the presence of **ZnPcTS** (10 μM) in water and with 4 eq. NaOH. To quantify the **ABMA** decay, the intensity of the emission peak at ~ 430 nm was tracked over the fifteen minutes to yield values corresponding to percentage of **ABMA** decayed. Plotting the relative intensities of this **ABMA** emission peak over time yields information relating to the rate of SO generation along with the associated kinetics. **Fig. 8A** displays **ABMA** decay plots of **ZnPcTS** (10 μM) , one with 4 eq. NaOH (blue line) and one with no NaOH in water (red line). The SO generation of **ZnPcTS** both with and without base in aqueous media is modest, with roughly a 10% decrease in **ABMA** intensity after 15 minutes. A control **ABMA** plot without any **ZnPcTS** is also shown in **Fig. 8A**, as there is a small inherent decay of **ABMA** fluorescence over time. Again, this poor SO generation rate is largely a consequence of the significant aggregation in the aqueous solvent.

CTAB was shown to decrease **ZnPcTS** aggregation at a concentration of 1 μM in aqueous solution. This is corroborated by the SO generation of **ZnPcTS** in said system (**Fig. S2**). Whilst the effect is relatively small, an increase in SO generation over fifteen minutes is observed. Similarly to the fluorescence quenching of **ZnPcTS** by **CTAB**, the fluorescence of **ABMA** is also completely quenched by the addition of 10 μM **CTAB**, prohibiting SO generation measurements with this probe.

Fig. 8A also shows **ABMA** decay plots of **ZnPcTS_0EqBase@Gel** and **ZnPcTS_4EqBase@Gel** dispersed in water. An enhancement in SO-generating ability is clearly seen for both gels tested, **Fig. S3** shows the fluorescence emission decay of **ABMA** for the measurements with **ZnPcTS_4EqBase@Gel**, where a clear qualitative difference can be seen in comparison with **Fig. S1**. Fitting pseudo first order kinetics results in a rate enhancement (with respect to aqueous solution) of 17x and 9x for **ZnPcTS_4EqBase@Gel** and **ZnPcTS_0EqBase@Gel**, respectively. Whilst encapsulation in the **1.2Br** gel clearly enhances SO generation, a disparity between **ZnPcTS_4EqBase@Gel** and **ZnPcTS_0EqBase@Gel** exists. Increased aggregation of **ZnPcTS** within the gel containing no NaOH, along with a potential influence of the heavy atom effect may be contributing to this difference. This disparity is explained by the observed reduced fluorescence of **ZnPcTS_4EqBase@Gel** compared with **ZnPcTS_0EqBase@Gel**. With the triplet excited state of the former being stabilised by the heavy atom effect, fluorescence should decrease as a result in more intersystem crossing, which we observe as enhanced SO generation. To further test the effect of NaOH, similar measurements were obtained for **ZnPcTS@Gels** containing 1, 2, and 3 equivalents of NaOH. **Fig. 8B** shows the **ABMA** decay curves for **ZnPcTS@Gels** with 0 to 4 equivalents of base. Largely within error, the **ZnPcTS_1,2,3EqBase@Gels** yield **ABMA** decay curves that lie in between that of **ZnPcTS_0EqBase@Gel** and **ZnPcTS_4EqBase@Gel**, indicating that increasing NaOH content induces an increase in SO generation through gradual disaggregation.

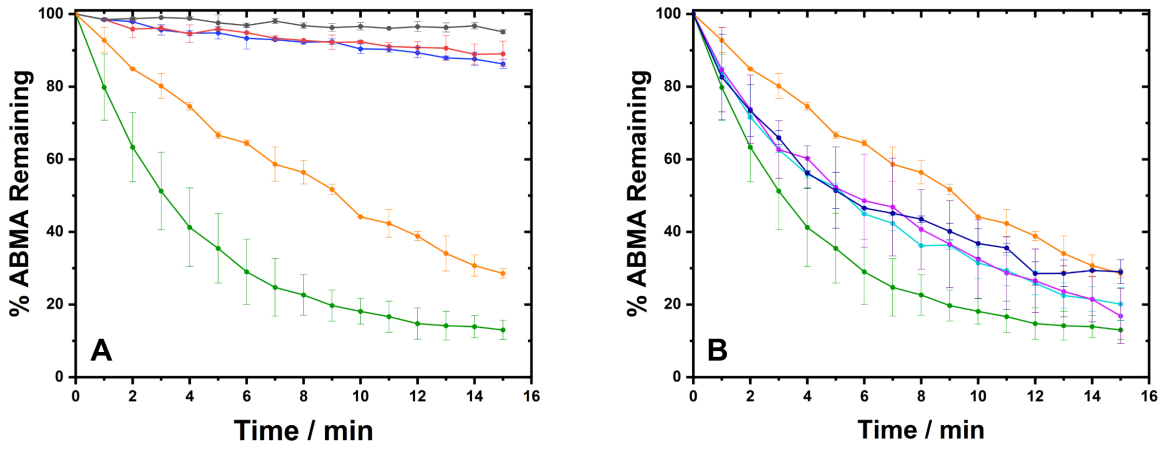

Fig. 8. (**A**) **ABMA** decay plot without **ZnPcTS** (grey line), **ZnPcTS** (10 μM) with no NaOH (red line) in aqueous solution, **ZnPcTS** (10 μM) with 4 eq. NaOH (blue line) in aqueous solution, **ZnPcTS_0EqBase@Gel** (orange) and **ZnPcTS_4EqBase@Gel** (green) (**B**) **ABMA** decay plot of **ZnPcTS_0Eq** (orange), **ZnPcTS_1EqBase@Gel** (cyan), **ZnPcTS_2EqBase@Gel** (dark blue), **ZnPcTS_3EqBase@Gel** (magenta), and **ZnPcTS_4EqBase@Gel** (green). In all gel samples, final [**ZnPcTS**] = 2 μM.

CONCLUSION

Aggregation of **ZnPcTS** in aqueous solution has been shown to considerably quench SO generation. In a mixed water-ethanol solvent system, the water-soluble phthalocyanine predominantly exists in its unaggregated form. The creation of a water-ethanol microenvironment within an excess of water through dispersion of a water-ethanol **1.2Br** gel has allowed the photosensitizer to retain its non-aggregated form and subsequently possess the ability to generate a significantly increased amount of SO compared with the same phthalocyanine in aqueous solution. The presence of base has also been shown to affect **ZnPcTS** aggregation both in aqueous solution and as part of the gel by limiting aggregation. This study demonstrates the effectiveness of supramolecular encapsulation in soft materials for realising the potential of water-soluble photosensitizers that are highly susceptible to aggregation in aqueous environments.

Acknowledgements

Project PID2020-115663GB-C32 was funded by MCIN/AEI. SMS thanks the University of Nottingham through the Beacon of Excellence Propulsion Futures and the EPSRC through the LDMI DTP for funding. DBA thanks the Ministerio de Ciencia e Innovación for funding through project PID2021-123873NB-I00.

REFERENCES

1. de la Torre G, Claessens CG, Torres T. *Chem. Commun*. 2007; 2000-2015.
2. Bottari G, de la Torre G, Guldi DM, Torres T. *Coord. Chem. Rev*. 2021; **428**: 213605.

3. Urbani M, Ragoussi M-E, Nazeeruddin MK, Torres T. *Coord. Chem. Rev*. 2019; **381**: 1-64.
4. Cid J-J, Yum J-H, Jang S-R, Nazeeruddin MK, Martinez-Ferrero E, Palomares E, Ko J, Graetzel M, Torres T. *Angew. Chem., Int. Ed*. 2007; **46**: 8358-8362.
5. Urbani M, de la Torre G, Nazeeruddin MK, Torres T. *Chem. Soc. Rev*. 2019; **48**: 2738-2766.
6. Bottari G, de la Torre G, Torres T. *Acc. Chem. Res*. 2015; **48**: 900-910.
7. Ragoussi M-E, Torres T. *Chem. Asian. J*. 2014; **9**: 2676-2707.
8. Bottari G, de la Torre G, Guldi DM, Torres T. *Chem. Rev*. 2010; **110**: 6768-6816.
9. İşci Ü, Dumoulin F. Fundamentals of Porphyrin Chemistry : A 21st Century Approach, vol. 1. Eds Brothers and Senge: 2022; Chapter 5.
10. Almeida-Marrero V, van de Winckel E, Anaya-Plaza E, Torres T, de la Escosura. *A. Chem. Soc. Rev*. 2018: **47**: 7369-7400.
11. Lo P-C, Rodriguez-Morgade MS, Ng DKP, Torres T, Pandey R, Dumoulin F. *Chem. Soc. Rev*. 2020; **49**: 1041-1056.
12. Pontón I and Sánchez-García D. *J. Porphyrins Phthalocyanines*. 2021; **25**: 917-929.
13. Dumoulin F, Durmus M, Ahsen V, Nyokong T. *Coord. Chem. Rev*. 2010; **254**: 2792-2847.
14. Cauchon N, Tian H, Langlois R, La Madeleine C, Martin S, Ali H, Hunting D, van Lier JE. *Bioconjugate Chem*. 2005; **16**: 80-89.
15. van Lier JE, Tian H, Ali H, Cauchon N, M. Hasséssian HM. *J. Med. Chem*. 2009; **52**: 4107–4110.
16. Ikeuchi T, Mack J, Nyokong T, Kobayashi N, Kimura M. *Langmuir*. 2016; **32**: 11980–11985.
17. Nyokong T. *Coord. Chem. Rev*. 2007; **251**: 1707–1722.
18. Zakir M, Khurshid A, Khan MI, Khattak A, Khan MA. *J. Porphyrins Phthalocyanines*, 2021; **25**: 102-119.
19. Baek SY, Na K. *Colloids Surf. B*. 2013; **101**: 493-500.
20. Chen B, He C, Song W, Zhao C, Gao Y, Chen Z, Dong Y, Wu Y, Li R. *RSC Adv*. 2015; **5**: 55150-55157.
21. El-Khouly ME, Kobaisy AM, Sallam G, Yoshihisa M. *J. Porphyrins Phthalocyanines*, 2022; **26**: 132-139.
22. Pashkovskaya AA, Maizlish VE, Shaposhnikov GP, Kotova EA, Antonenko YN. *Biochim. Biophys. Acta - Biomembr*. 2008; **1778**: 541-548.
23. Urizzi P, Allen CM, Langlois R, Ouellet R, La Madeleine C, Van Lier JE. *J. Porphyrins Phthalocyanines* 2001; **5**: 154-160.
24. Rodrigues M, Calpena AC, Amabilino DB, Garduño-Ramírez ML, Pérez-García L. *J. Mater. Chem. B*. 2014; **2**: 5419-5429.
25. Limón D, Gil-Lianes P, Rodríguez-Cid L, Alvarado HL, Díaz-Garrido N, Mallandrich M, Baldomà, Calpena AC, Concepción D, Aliaga-Alcade N, González-Campo A, Pérez-García L. *ACS Appl. Nano Mater*. 2022; **5**: 13829-13839.
26. Samperi M, Bdiri B, Sleet CD, Markus R, Mallia AR, Pérez-García L, Amabilino DB. *Nat. Chem*. 2021; **13**: 1200-1206.
27. Samperi M, Limón D, Amabilino DB, Pérez-García L. *Cell Rep. Phys. Sci*. 2020; **1**: 100030.
28. Casal-Dujat L, Rodrigues M, Yagüe A, Calpena A, Amabilino DB, González-Linares J, Borràs M, Pérez-García L. *Langmuir*. 2012; **28**: 2368-2381.

29. Limón D, Domínguez KT, Garduño-Ramírez ML, Andrade B, Calpena A, Pérez-García L. *Colloids Surf. B*. 2019; **181**: 657-670.
30. Dong H, Du H, Wickramasinghe SR, Qian X. *J. Phys. Chem. B*. 2009; **113**: 14094–14101.
31. Guthrie JP. *Can. J. Chem*. 1978; **56**: 17.
32. Li X-Y, He X, Ng ACH, Wu C, Ng DKP. *Macromolecules*. 2000; **33**: 2119-2123.
33. Wolf T, *Ber. Bunsenges. Phys. Chem*. 1982; **86**: 1132-1134.
34. Nakai K, Usami J, Kobayashi N. *J. Porphyrins Phthalocyanines*. 2007; **11**: 222-227.
35. Yin H, Wang M, Tan LS, Chiang LY, *Molecules*. 2019; **24**: 3337.

Supramolecular and base-induced singlet oxygen generation enhancement of a water-soluble phthalocyanine

Shaun M. Smith, Thais F. Abelha, David Limón, Mario Samperi, Bunty Sharma, Kristjan Plaetzer, Fabienne Dumoulin, David B. Amabilino, Lluïsa Pérez-García

Zinc(II) phthalocyanine tetrasulfonic acid was encapsulated into an imidazolium gel. When the phthalocyanine was incorporated with 4 equivalents of NaOH, the reduced aggregation brought about a greater amount of singlet oxygen generation compared with the phthalocyanine in aqueous solution when irradiated with red light. Singlet oxygen generation was measured through the fluorescence decay of an anthracene derivative molecular probe.